J Appl Biol Chem (2022) 65(4), 277–286
https://doi.org/10.3839/jabc.2022.036

Online ISSN 2234-7941
Print ISSN 1976-0442

Article: Bioactive Materials

Protective effects of quercetin-3-glucosyl-(1-2)-rhamnoside from *Schizophragma hydrangeoides* leaves on ultraviolet A-induced photoaging in human dermal fibroblasts

So Yeon Oh · Sung Chun Kim · Ho Bong Hyun · Hyejin Hyeon · Boram Go · Yong-Hwan Jung · Young-Min Ham

Received: 30 September 2022 / Accepted: 21 October 2022 / Published Online: 31 December 2022

Abstract *Schizophragma hydrangeoides* (*S. hydrangeoides*) is a vine endogenous to Jeju Island and Ulleungdo, where it grows attached to the foothills and rock surfaces. Previous research has mostly focused on the whitening effect of *S. hydrangeoides* leaf extract. In this study, we investigated *S. hydrangeoides* leaf extract further, and detected four phytochemicals in the extract: chlorogenic acid, quercetin-3-*O*-glucosyl-(1-2)-rhamnoside, quercetin-3-*O*-xylosyl-(1-2)-rhamnoside, and quercitrin. We pretreated human dermal fibroblast (HDFn) cells with previously established concentrations of the four compounds for 1 h before ultraviolet A (UVA) irradiation. Among the four compounds, quercetin-3-O-glucosyl-(1-2)-rhamnoside (Q-3-GR) best inhibited matrix metalloproteinase-1 (MMP-1) levels. Thus, we investigated the protective effects of Q-3-GR on photoaging and its underlying mechanisms. Q-3-GR significantly reduced MMP-1 production and inhibited MMP-1 protein expression in UVA-irradiated HDFn cells. Furthermore, Q-3-GR increased procollagen type I production and protein expression. Q-3-GR exerted its anti-photoaging effects by downregulating the mitogen-activated protein kinase/ activator protein-1 signaling pathway, and upregulating the transforming growth factor-β/Smad signaling pathway. Thus, *S. hydrangeoides* leaf-derived Q-3-GR is a potential potent cosmetic ingredient for UV-induced skin aging.

Keywords Collagen · Matrix Metalloproteinase-1 · Mitogen-activated Protein Kinases

Introduction

Skin aging is a normal phenomenon of human aging that alters skin function and appearance by intrinsic or chronological causes, and extrinsic aging. Intrinsic aging occurs naturally with advancing age, while the environmental factor primarily responsible for causing extrinsic aging is photoaging [1-3]. Ultraviolet (UV) radiation is divided into UVA, UVB, and UVC subtypes, based on their wavelengths. UVA (320-400 nm) comprises more than 90% of the UV that skin is exposed to, while some UVB (280-320 nm) and almost all UVC (100-280 nm) are absorbed by the ozone layer. Since UVB has a shorter wavelength than UVA, it does not reach the skin dermis. Thus, UVA is primarily responsible for epidermal photoaging as it can reach the dermal layer of the skin [4,5]. The dermis contains fibrous proteins, such as collagen, and elastic fibers, called the extracellular matrix (ECM) [6], which provide elasticity and strength to the skin. UVA causes skin wrinkles by contributing to the denaturation and decomposition of collagen and elastic fibers [7,8].

Disruption of the skin collagen matrix by UV occurs due to stimulation of collagen degradation as well as inhibition of procollagen production [9]. Exposure of the skin to UVA causes oxidative stress due to the generation of intracellular reactive oxygen species (ROS), which activates the mitogen-activated protein kinase (MAPK) signaling pathway, including extracellular signal-regulated kinases (ERK), c-Jun N-terminal kinases (JNK), and p38 kinase. The phosphorylation of MAPKs activated activator protein-1 (AP-1), which is part of the c-Fos-c-Jun heterodimer complex [10-12]. Activated AP-1 increased the production of

So Yeon Oh and Sung Chun Kim are contributed equally to this work.

Young-Min Ham (✉)
E-mail: hijel@jejutp.or.kr

Biodiversity Research Institute, Jeju Technopark, Seagwipo, Jeju 63068, Republic of Korea

matrix metalloproteinases (MMPs), such as MMP-1 (collagenase-1), which led to the degradation of collagen and elastin fibers [13,14]. Procollagen was produced through the transforming growth factor-β (TGF-β)/Smad signaling pathway, and UV irradiation downregulated this pathway by regulating Smads. Phosphorylated receptor-regulated Smad (R-Smad) containing Smad 2 and 3, formed a heterodimer complex with the common mediator Smad (Co-Smad), such as Smad 4. This complex translocates to the nucleus and induces procollagen synthesis [3,15,16]. Therefore, identifying natural compounds that prevent collagen degradation and induce procollagen production is important to prevent photoaging.

Schizophragma hydrangeoides is a vine endogenous to Jeju Island and Ulleungdo, and a previous study reported that a 70% ethanol extract of *S. hydrangeoides* had a whitening effect [17]. However, the anti-photoaging effects of *S. hydrangeoides* extract are unknown. Herein, we report that quercetin-3-glucosyl-(1-2)-rhamnoside (Q-3-GR) isolated from *S. hydrangeoides* leaf extracts mediates anti-photoaging effects, and describe the underlying molecular mechanisms involved.

Materials and Methods

Chemicals and Reagents

Ethanol was purchased from Samchun Chemicals (Seoul, South Korea). *n*-Hexane, chloroform, ethyl acetate, and *n*-butanol were purchased from Daejung Chemicals (Siheung, Gyeonggi-do, Republic of Korea). Sephadex LH-20 and methanol were purchased from GE Healthcare (Chicago, IL, USA) and Cambridge Isotope Laboratories Inc. (Tewksbury, MA, USA), respectively. Dulbecco's modified Eagle's medium (DMEM), Ham's F-12 Nutrient Mix, penicillin/streptomycin, trypsin-ethylenediaminetetraacetic acid, heat-inactivated fetal bovine serum (FBS), and bicinchoninic acid (BCA) protein kits were purchased from Thermo Fisher Scientific (Waltham, MA, USA). The MMP-1 human ELISA kit was purchased from Abcam (Cambridge, UK), and the Procollagen type I C-peptide (PIP) EIA kit was purchased from Takara (Tokyo, Japan). The protease inhibitor cocktail and anti-collagen primary antibody were purchased from Sigma-Aldrich (St. Louis, MO, USA). Phosphatase/protease inhibitor cocktail, primary antibodies (MMP-1, P-ERK, P-JNK, P-p38, P-c-Jun, P-c-Fos, P-Smad 2/3, ERK, JNK, p38, c-Jun, c-Fos, Smad 2/3, Smad 4, and β-actin), and anti-mouse and anti-rabbit secondary antibodies were purchased from Cell Signaling Technology (Danvers, MA, USA). 3-(4,5-dimethylthiazol-2-yl)-2,5-diphenyltetrazolium bromide (MTT), dimethyl sulfoxide (DMSO), and tris-buffered saline (TBS) were purchased from Biosesang (Seongnam, Korea). ECL solution was purchased from iNtRON Biotechnology (Sungnam, Gyeonggi-do, Korea).

Extraction and Isolation

S. hydrangeoides leaves were collected in May 2021 near the Muljangol Bridge on Jeju Island, Korea. To identify the active compounds, dried powdered leaves (600 g) of *S. hydrangeoides* were extracted thrice with 70% ethanol and water for 24 h at room temperature. The resulting ethanol solution was combined and filtered. The filtrate was concentrated using a rotary evaporator at 37 °C to obtain 143 g extract. A portion of the extract (100 g) was suspended in water, and successively fractionated into *n*-hexane, chloroform, ethyl acetate, *n*-butanol, and water fractions. The *n*-butanol layer was fractionated using medium-pressure liquid chromatography (MPLC, Buchi, Flawil, Switzerland) on a C18 column with a water-methanol gradient to obtain 60 fractions (MP1-MP60). Fraction MP51 was identified as compound 2 (120 mg), and fractions MP16-19 were purified by Sephadex LH-20 column chromatography (CC) with methanol to isolate compound 1 (38 mg). Fraction MP53 was subjected to Sephadex LH-20 CC with chloroform-methanol (2:1) to obtain compounds 3 (14 mg) and 4 (10 mg). The separated compounds were structurally identified using a nuclear magnetic resonance (NMR) system (JEOL, Tokyo, Japan). ^{1}H and ^{13}C NMR were measured at 400 and 100 MHz, respectively, using methanol-d4 (δ_H 3.31 and δ_C 49.1 ppm) as NMR solvent.

Cell Culture and UVA Irradiation

Human dermal fibroblast (HDFn) cells were cultured in DMEM/F-12 (3:1), supplemented with 10% FBS and 1% penicillin/streptomycin at 37 °C and 5% CO_2 in a humidified atmosphere. Cells were exposed to a Bio-Link UV irradiation system (Vilber Lourmat, Collegien, France) equipped with UVA sources. The cells were washed with PBS and covered with PBS until they were slightly submerged. The cells were exposed to UVA until 8 J/cm^2. PBS was replaced with fresh serum-free medium after UVA irradiation, and the experiments were performed.

Cell Viability

HDFn cells were seeded in 24-well plates at a density of 7×10^4 cells/well and cultured for 24 h. After washing once, the cells were treated with compounds 1-4 at the indicated concentrations in serum-free media and incubated for 48 h. The supernatant was removed and 500 μL of MTT reagent (0.4 mg/mL in serum-free media) was added per well, and incubated for 4 h. After removing the MTT reagent, DMSO was added to dissolve the formed formazan crystals, and the absorbance was measured at 570 nm using a microplate reader (Tecan, Salzburg, Austria).

Enzyme-Linked Immunosorbent Assay (ELISA)

HDFn cells were seeded in a 24-well plate at 7×10^5 cells/well and incubated for 24 h. Cells were pretreated with compounds 1-4 at the indicated concentrations, adenosine (100 μM), and ascorbic acid

(100 μM) for 1 h. Adenosine was used as a positive control for MMP-1 production, and ascorbic acid was used as a positive control for procollagen type I production. After UVA irradiation, the cells were treated with the four compounds at the indicated concentrations for 48 h, and the cell supernatant was collected to measure MMP-1 and PIP using ELISA kits. MMP-1 and PIP ELISA assays were performed according to the manufacturers' protocols.

Western Blot

HDFn cells were seeded in 6-well plates at 3×10^5 cells/well and incubated for 24 h, followed by pretreatment with Q-3-GR (5, 10, and 20 μM) for 1 h. After UV irradiation, the cells were treated with Q-3-GR (5, 10, and 20 μM) to measure protein levels at different time points. After washing with cold 1× PBS, cell lysates were prepared using RIPA buffer containing a 1% protease/phosphatase inhibitor cocktail. Lysis was performed at 4 °C for 20 min. Cells were collected in a 1.5 mL tube, centrifuged at 15,000 rpm for 20 min at 4 °C to obtain the supernatants. Protein concentration was quantified using a BCA protein assay kit. The loading samples were prepared using sample buffer and heated at 100 °C for 5 min to denature the proteins. The protein samples were subjected to electrophoresis on sodium dodecyl sulfate-polyacrylamide gels to separate proteins by size. The separated proteins were transferred from the gel to a polyvinylidene fluoride membrane. After blocking in blocking buffer for 1 h, the membranes were incubated with the primary antibody at 4 °C for more than 20 h. The membranes were then washed four times for 5 min each with 1x TBS-T, followed by incubation with the secondary antibody diluted in 1× TBS-T at room temperature for 1 h. The membranes were washed four times for 5 min each, incubated with the ECL solution, followed by protein detection using ChemiDoc (Vilber Lourmat, Collegien, France).

Statistical Analysis

The results of all experiments are expressed as mean ± standard deviation (mean ± SD) of three independent experiments. Statistical differences were calculated using one-way analysis of variance (ANOVA) to compare the control and treatment groups. Statistical analysis was performed using Winks statistics software (TexaSoft, Plano, TX, USA).

Results

Identification of Compounds Using NMR

We used chromatography purification to isolate four known compounds, 1-4, and confirmed their chemical structures by analyzing the NMR spectroscopic data. Compound 1 showed 16 signals in the ^{13}C NMR spectrum, where eight sp^2 carbons, four oxygen-bearing sp^3 carbons and two carbonyl carbons were identified. The presence of two CH_2 groups was indicated based on the ^{1}H (2.17-1.96, 4H, m, H-2', H-6') and ^{13}C NMR signals (39.2 and 40.7 ppm) (Table 1). We confirmed compound 1 to be chlorogenic acid (MW: 354.31 g/mol) by comparing the obtained data with previously established values [18]. Compounds 2, 3, and 4 showed typical flavonoid derivative signals in their ^{1}H and ^{13}C NMR spectra. The ^{1}H NMR signals of compound 2 indicated the presence of quercetin aglycone. This was confirmed by two doublet signals at δ 6.92 (1H, d, J=8.2 Hz) and 7.35 (1H, d, J=2.3 Hz), assigned to H-5' and H-2', respectively, and a *dd* signal at δ 7.32 (H-6'). The presence of H-6 and H-8 was identified by two doublet signals at δ 6.20 and 6.37. In the ^{1}H-NMR spectrum, peaks at δ 4.38 (1H, d, J=7.8 Hz) and 5.64 (1H, brs) indicate specific peaks of glucose and rhamnose, respectively. Based on previous literature, we identified compound 2 as quercetin-3-*O*-glucosyl-(1-2)-rhamnoside (MW: 610.52 g/mol) [19]. The ^{13}C NMR spectrum of compound 3 was similar to that of compound 2, except for the presence of eleven sugar carbon signals (Table 2). Thus, we identified compound 3 as quercetin with combined xylose and rhamnose, and established it as quercetin-3-*O*-xylosyl-(1-2)-rhamnoside (MW: 580.14 g/mol) based on previous literature [20]. Similarly, we confirmed compound 4 to be quercetin with rhamnose, identified as quercitrin (MW: 448.38 g/mol) [21]. This is the first study to isolate these compounds from *S. hydrangeoides*.

Table 1 ^{1}H-NMR and ^{13}C-NMR chemical shifts of compound **1** in CD_3OD

Position	Compound **1**	
	δ_H (multi; J [Hz])	δ_C
1		127.8
2	7.03 (d, J=1.8 Hz)	115.8
3		146.8
4		149.6
5	6.77 (d, J=8.2 Hz)	116.8
6	6.93(dd, J=1.8, 7.8 Hz)	123.1
7	7.56 (d, J=16.0 Hz)	146.9
8	6.29 (d, J=16.0 Hz)	115.3
9		169.1
1'		77.8
2'	2.17–1.96 (m)	39.2
3'	5.37 (m)	75.1
4'	4.13 (brs)	73.1
5'	3.69 (dd, J=10.0, 3.2 Hz)	72.6
6'	2.17-1.96 (m)	40.7
7'		180.8

Effects of Compounds Isolated from *S. hydrangeoides* on MMP-1 Production and Cell Viability in HDFn cells

We compared the effects of all four compounds isolated from *S. hydrangeoides* to determine their efficacy in preventing photoaging: (a) chlorogenic acid, (b) quercetin-3-*O*-glucosyl-(1-2)-rhamnoside, (c) quercetin-3-*O*-xylosyl-(1-2)-rhamnoside, and (d) quercitrin (Fig. 1).

Table 2 ^{1}H-NMR and ^{13}C-NMR chemical shifts of compound **2-4** in CD_3OD

Position	Compound **2**		Compound **3**		Compound **4**	
	δ_H (multi; *J* [Hz])	δ_C	δ_H (multi; *J* [Hz])	δ_C	δ_H (multi; *J* [Hz])	δ_C
2		159.3		159.2		159.5
3		136.6		136.9		136.4
4		179.6		179.9		179.8
5		163.2		163.3		163.4
6	6.20 (*d*, *J* =2.1 Hz)	100	6.19 (*d*, *J* =2.1 Hz)	99.9	6.20 (*d*, *J* =2.1 Hz)	100
7		166.3		166		166.1
8	6.37 (*d*, *J* =2.3 Hz)	94.9	6.36 (*d*, *J* =2.3 Hz)	94.9	6.37 (*d*, *J* =2.3 Hz)	94.9
9		158.6		158.6		158.7
10		106		105.9		106
1'		122.9		122.9		123.1
2'	7.35 (*d*, *J* =2.3 Hz)	117	7.35 (*d*, *J* =2.3 Hz)	116.9	7.34 (*d*, *J* =2.3 Hz)	117.1
3'		146.6		146.6		146.6
4'		150		150		150
5'	6.92 (*d*, *J* =8.2 Hz)	116.6	6.92 (*d*, *J* =8.2 Hz)	116.6	6.91 (*d*, *J* =8.2 Hz)	116.5
6'	7.32 (*d*, *J* =2.1, 8.2 Hz)	122.9	7.30 (*d*, *J* =2.1, 8.2 Hz)	122.8	7.32 (*d*, *J* =2.1, 8.2 Hz)	123
1"	5.64 (brs)	102.7	5.34 (brs)	103.4	5.34 (brs)	103.7
2"		83		82.9		72.3
3"		72.1		72		72.2
4"		73.6		73.8		73.4
5"		70.8		71.1		72.1
6"	0.98 (*d*, *J* =6.4 Hz)	17.8	1.02 (*d*, *J* =5.9 Hz)	17.8	0.93 (*d*, *J* =5.9 Hz)	17.8
1'''	4.38 (*d*, *J* =7.8 Hz)	107.3	4.24 (*d*, *J* =7.3 Hz)			
2'''		75.4				
3'''		77.9				
4'''		71.9				
5'''		70.8				
6'''		62.3				
1"				107.9		
2"				75.4		
3"				77.9		
4"				71.9		
5"				67.2		

We observed that, of the four compounds, quercetin-3-glucosyl-(1-2)-rhamnoside (Q-3-GR) inhibited MMP-1 production the most at non-toxic concentrations (Table 3). Thus, we focused on investigating the effects of Q-3-GR on inhibiting collagenase and enhancing collagen production, along with the related signaling pathways.

Effects of Q-3-GR on MMP-1 expression in UVA-irradiated HDFn cells

UV irradiation induces collagen degradation by causing overexpression of MMP-1. Therefore, reducing MMP-1 levels is a key factor in preventing UVA-induced photoaging [22]. We investigated the effects of Q-3-GR on MMP-1 production and protein expression using ELISA and western blotting. UVA irradiation significantly increased MMP-1 production (Fig. 2), and decreased adenosine levels by 45.3±9.7%. Treatment with Q-3-GR decreased MMP-1 production by 48.7±7.2, 53.7±4.5, and 74.8±2.5% at 5, 10, and 20 μM, respectively (Fig. 2A). Western blotting revealed that Q-3-GR decreased MMP-1 protein expression by 50% at 20 μM compared to the UVA-irradiation group (Fig. 2B).

Effects of Q-3-GR on procollagen type I expression in UVA-irradiated HDFn cells

Skin collagen is responsible for ECM structure and contributes to skin elasticity [23]. Therefore, we performed ELISA and western blotting to investigate the effects of Q-3-GR on procollagen type I production and protein expression upon UVA-induced photoaging. As expected, UVA decreased the production of procollagen type I,

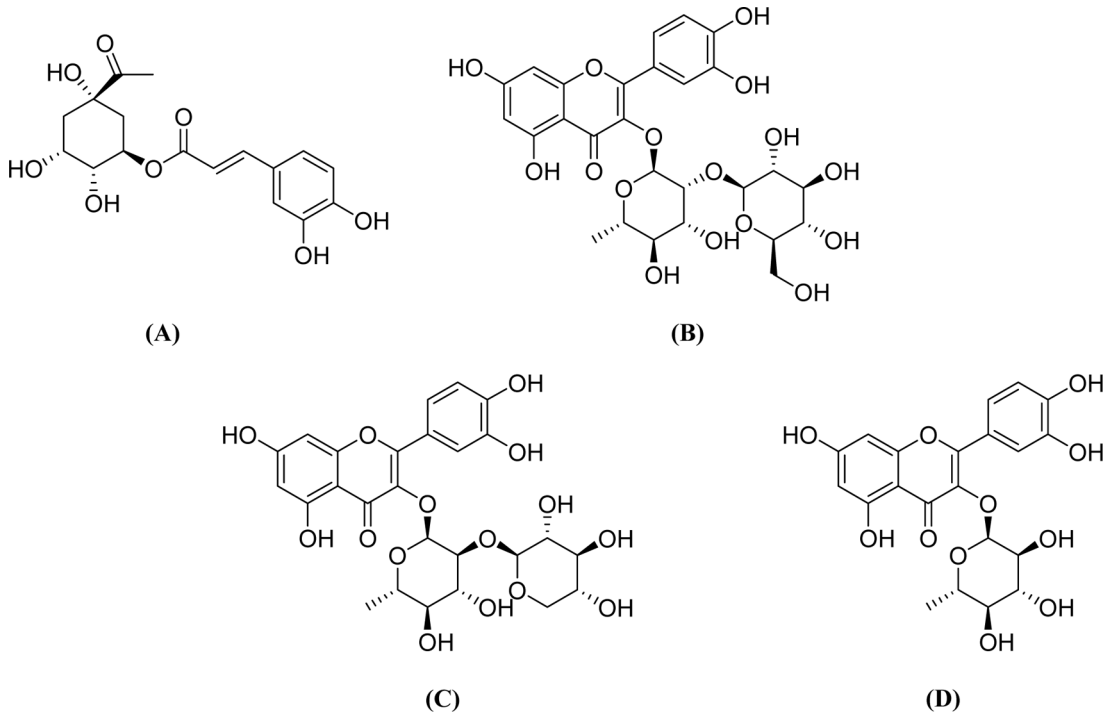

Fig. 1 Structures of isolated compounds from *S. hydrangeoides*; (A) chlorogenic acid; (B) quercetin-3-*O*-glucosyl-(1-2)-rhamnoside; (C) quercetin-3-*O*-xylosyl-(1-2)-rhamnoside; and (D) quercitrin

Table 3 Effects of *S. hydrangeoides* compounds on MMP-1 production and the viability of HDFn cells

No.	Compound	Concentration (μM)	MMP-1 production (%)	Cell viability (%)
1	Chlorogenic acid	10	76.6	96.8
		20	65.2	103.5
		40	67.6	100.7
2	Quercetin-3-glucosyl-(1-2)-rhamnoside	5	51.3	95.0
		10	46.3	92.2
		20	25.2	90.7
3	Quercetin-3-xylosyl-(1-2)-rhamnoside	5	48.5	73.0
		10	35.5	55.1
		20	23.7	45.7
4	Quercitrin	10	50.2	98.3
		20	42.0	101.0
		40	32.6	104.9

while vitamin C (positive control) treatment increased procollagen type I levels by 38.4±5.7%. Q-3-GR treatment increased procollagen type I production by 13.7±4.9, 44.2±7.0, and 59.2±1.0% at 5, 10, and 20 μM, respectively (Fig. 3A). Moreover, western blotting revealed that Q-3-GR treatment also increased procollagen type I protein expression in a concentration-dependent manner (Fig. 3B).

Effects of Q-3-GR on MAPK/AP-1 signaling pathway in UVA-irradiated HDFn cells

The MAPK signaling pathway is stimulated by ROS, resulting in activation of the AP-1 transcription factor, and formation of the c-Fos and c-Jun heterodimer complex. Activated AP-1 stimulates the production of MMPs, which in turn induces collagen degradation [24,25]. Thus, we performed western blotting to investigate the effect of Q-3-GR on the MAPK/AP-1 signaling pathway. As shown in Fig. 4A, UVA irradiation induced phosphorylation of ERK, JNK, and p38. Q-3-GR treatment reduced the expression of p-ERK in a concentration-dependent manner (Fig. 4B), and significantly suppressed the expression of p-JNK (Fig. 4C). However, it did not inhibit the expression of p-p38 (Fig. 4D). Previous studies have shown that c-Jun and c-Fos are regulated by the MAPK signaling pathway. ERK and JNK are also involved in c-Fos and c-Jun regulation, respectively [26,27]. We observed markedly increased phosphorylation of c-Jun and c-Fos following UVA irradiation (Fig. 5A), while Q-3-GR treatment significantly inhibited c-Jun and c-

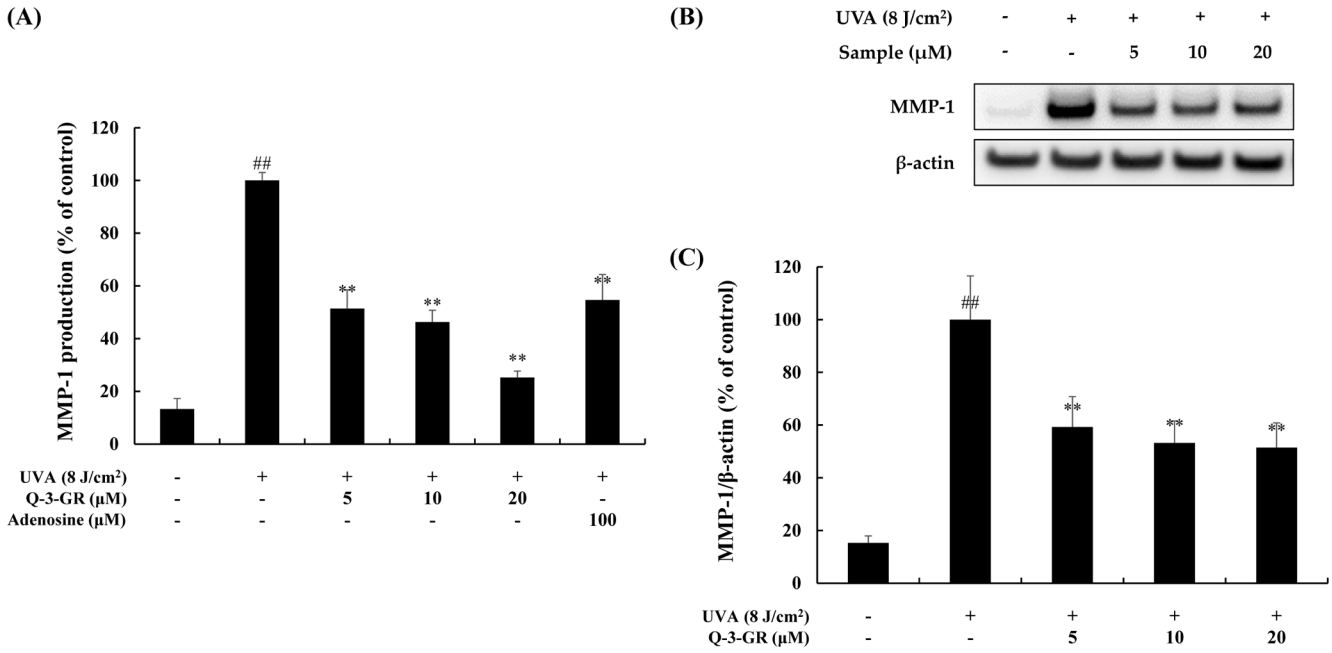

Fig. 2 Effects of Q-3-GR on MMP-1 production and protein expression in UVA-irradiated HDFn cells. The cells were pretreated with Q-3-GR (5, 10, and 20 μM) or adenosine (100 μM) for 1 h. After UVA irradiation, cells were incubated in the compounds for an additional 24 h. (A) MMP-1 inhibitory effect of Q-3-GR was measured by ELISA. Adenosine was used as a positive control. (B) Western blot results and (C) protein level of MMP-1. MMP-1 and β-actin (loading control) levels were quantified using Image J. Data are presented as mean ± SD (n =3). $^{\#\#}p$ <0.01 vs. non-treated control; $^{**}p$ <0.01 vs. UVA-irradiated group

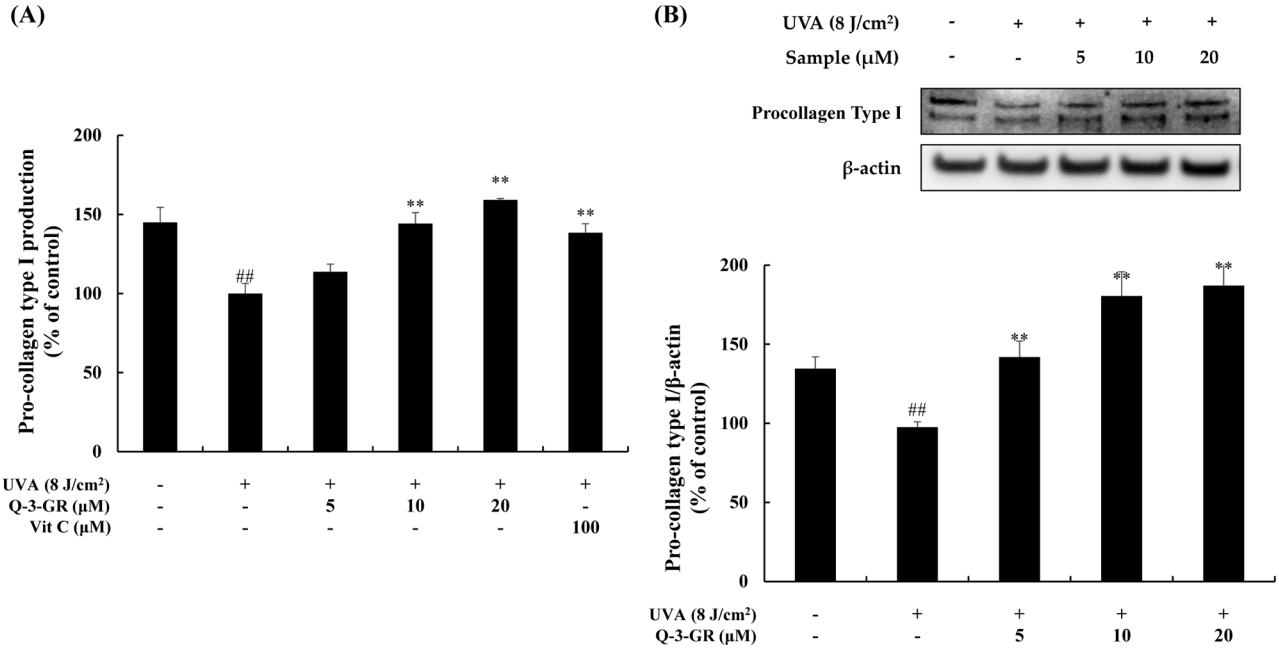

Fig. 3 Effects of Q-3-GR on procollagen type I production and protein expression in UVA-irradiated HDFn cells. The cells were pretreated with Q-3-GR (5, 10, and 20 μM) or vitamin C (100 μM) for 1 h. After UVA irradiation, cells were incubated with the compounds for an additional 24 h. (A) Effect of Q-3-GR on procollagen type I was measured by ELISA. Vitamin C was used as a positive control. (B) Western blot results and (C) protein levels of procollagen type I. Procollagen type I and β-actin (loading control) levels were quantified using Image J. Data are presented as mean ± SD (n =3). $^{\#\#}p$ <0.01 vs. non-treated control; $^{**}p$ <0.01 vs. UVA-irradiated group

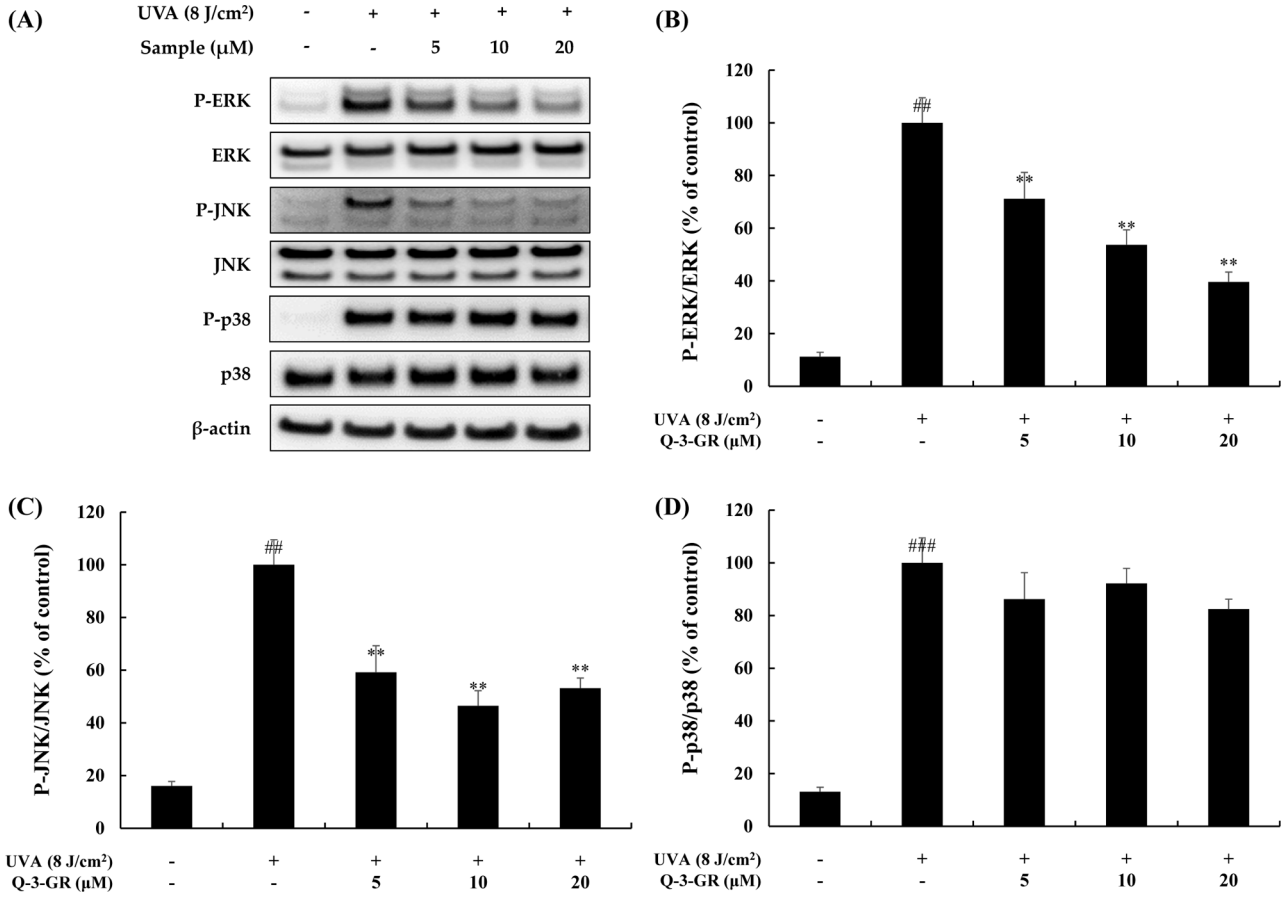

Fig. 4 Effect of Q-3-GR on the MAPK/AP-1 signaling pathway in UVA-irradiated HDFn cells. Western blotting results of (A) MAPK and protein levels of (B) P-ERK, (C) P-JNK, and (D) P-p38. The cells were pretreated with Q-3-GR (5, 10, and 20 μM) for 1 h. After UVA irradiation, cells were incubated with the compounds for an additional 1 h. Protein levels were quantified using Image J. Data are presented as mean ± SD (n =3). $^{\#\#}p$ <0.01 vs. non-treated control; $^{**}p$ <0.01 vs. UVA-irradiated group

Fos phosphorylation (Fig. 5B, 5C).

Effects of Q-3-GR on TGF-β/Smad signaling pathway in UVA-irradiated HDFn cells

TGF-β binds to its cell surface receptor to activate the TGF-β/Smad signaling pathway. Smad 2 and 3 form a complex with Smad 4, and regulate the transcription of target genes, such as collagen [3]. UV irradiation causes TGF-β receptor dysfunction to inhibit the TGF-β/Smad signaling pathway. As shown in Fig. 6, UVA irradiation decreased the phosphorylation of Smad 2/3, and the expression of Smad 4, while Q-3-GR treatment induced the expression of p-Smad 2/3 (Fig. 6B) and Smad 4 (Fig. 6C) in a concentration-dependent manner.

Discussion

With increasing life expectancy, there is increased interest in studying compounds that affect skin aging. Research is underway to identify new bioactive natural compounds to avoid side effects caused by chemical cosmetic components [28-30]. Thus, we attempted to identify phytochemicals with a preventive effect on photoaging. A previous study described the whitening effect of *S. hydrangeoides* extract [17]. However, its potential role in skin aging has remained unexplored, and there is no report on the anti-photoaging effects of Q-3-GR isolated from *S. hydrangeoides*. Therefore, we investigated these potential effects of Q-3-GR, as well as explored its mechanisms of action. We obtained four compounds from *S. hydrangeoides* leaves which were identified through NMR. We confirmed the MMP-1 production inhibitory activity of the four compounds, Q-3-GR (compound 2) had the best inhibitory effect at a non-toxic concentration. In subsequent experiments, we confirmed the effects of Q-3-GR on the expression of MMP-1 and procollagen type 1 through ELISA and western blot, and the mechanism was confirmed by western blot.

We isolated and identified four phytochemicals from the BuOH fraction of *S. hydrangeoides*, namely chlorogenic acid (compound 1), quercetin-3-*O*-glucosyl-(1-2)-rhamnoside (compound 2), quercetin-3-*O*-xylosyl-(1-2)-rhamnoside (compound 3), and quercitrin (compound 4). MMP-1 induced collagen breakdown in photoaging

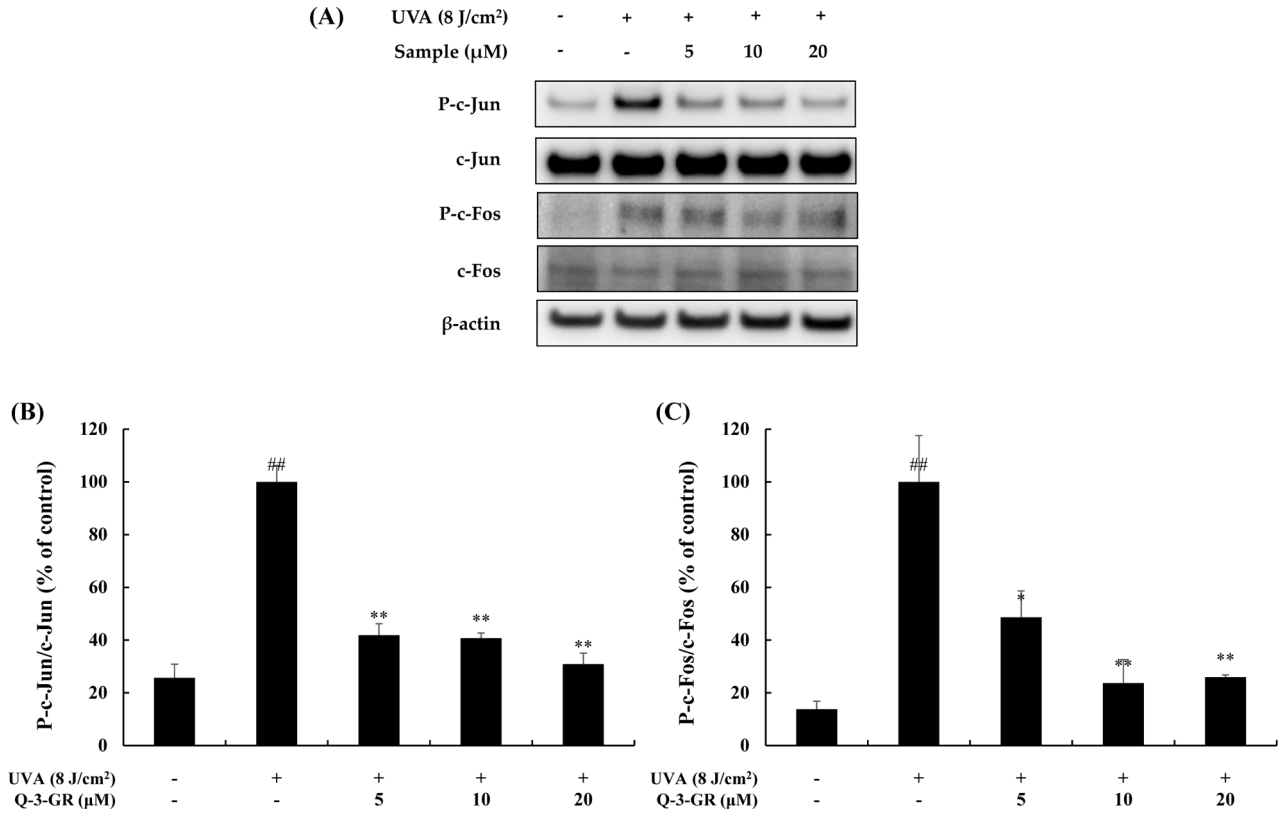

Fig. 5 Effect of Q-3-GR on the MAPK/AP-1 signaling pathway in UVA-irradiated HDFn cells. (A) Western blotting results and protein levels of (B) P-c-Jun and (C) P-c-Fos. The cells were pretreated with Q-3-GR (5, 10, and 20 μM) for 1 h. After UVA irradiation, cells were incubated with the compounds for an additional 24 h. Protein levels were quantified using Image J. Data are presented as mean ± SD (n =3). $^{\#\#}p$ <0.01 vs. non-treated control; $^{*}p$ <0.05 and $^{**}p$ <0.01 vs. UVA-irradiated group

skin [31], so we analyzed the MMP-1 production inhibitory activity of each compound to compare their anti-photoaging effects. As a result, Q-3-GR (compound 2) caused maximal inhibition of MMP-1 at a non-toxic concentration (Table 3). Therefore, we selected Q-3-GR for further analysis to investigate its protective effects on UVA irradiated-HDFn cells.

Procollagen type I is a precursor of collagen, which is the primary component of the ECM, and its breakdown results in skin wrinkles. MMP-1 degrades collagen, and decreased MMP-1 expression and increased procollagen type I expression contribute to skin elasticity [32,33]. ELISA and western blot analysis revealed that Q-3-GR decreased the production of MMP-1, and inhibited the expression of MMP-1 protein in UVA-irradiated HDFn cells (Fig. 2). Additionally, Q-3-GR increased procollagen levels and its protein expression in UVA-irradiated HDFn cells (Fig. 3). Therefore, our results showed that Q-3-GR prevents photoaging by reducing the production of MMP-1 and inducing the expression of procollagen type I.

The MAPK signaling pathway is activated by UV-induced ROS, which in turn activates the transcription of c-Jun and c-Fos, which form a heterodimer complex with AP-1. Activated AP-1 induces the expression of MMP-1 [24]. Western blotting revealed that Q-3-GR significantly inhibited ERK and JNK phosphorylation, but did not affect p38 phosphorylation, in addition to inhibiting c-Jun and c-Fos phosphorylation (Fig. 4, 5). These results demonstrated that Q-3-GR inhibits the activation of the MAPK/AP-1 signaling pathway by UVA irradiation, which results in blocking the production of MMP-1 and prevention of collagen degradation.

The TGF-β/Smad signaling pathway is involved in collagen synthesis. Smad 2/3 (R-Smad) forms a heteromeric complex with Smad 4 (Co-Smad), is translocated into the nucleus, and is involved in the synthesis of type I collagen [3]. We observed that Q-3-GR significantly increased the phosphorylation of Smad 2/3 and Smad 4 (Fig. 6). These results suggested that Q-3-GR activated the TGF-β/Smad signaling pathway and thereby increases collagen synthesis. In conclusion, Q-3-GR isolated from *S. hydrangeoides* inhibits the generation of MMP-1 through the MAPK/AP-1 signaling pathway and increases procollagen type I through the TGF-β/Smad signaling pathway in UVA-irradiated HDFn cells. Our study suggests that the naturally derived Q-3-GR has protective effects against photoaging and shows potential for use as an anti-photoaging agent in cosmetics.

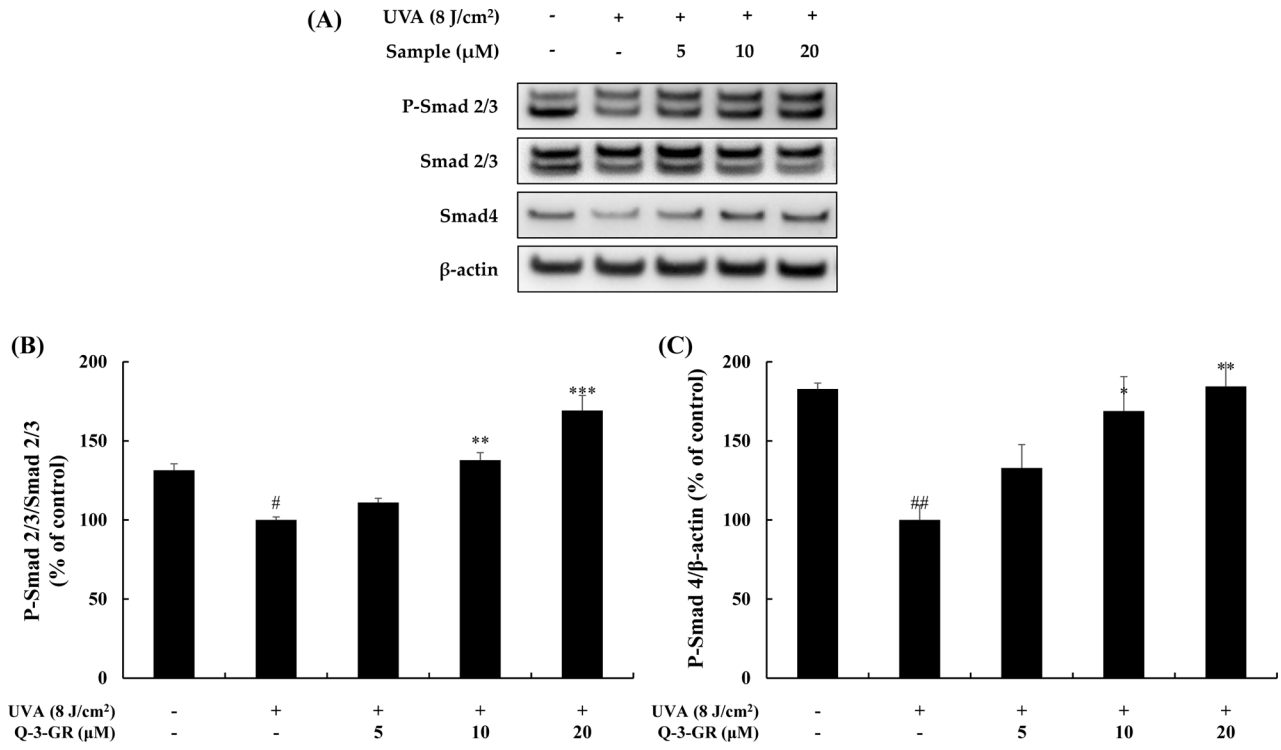

Fig. 6 Effect of Q-3-GR on the Smad signaling pathway in UVA-irradiated HDFn cells. (A) Western blotting results and protein levels of (B) P-Smad 2/3 and (C) Smad 4. The cells were pretreated with Q-3-GR (5, 10, and 20 μM) for 1 h. After UVA irradiation, cells were incubated with the compounds for an additional 24 h. Protein levels were quantified using Image J. Data are presented as mean ± SD (n =3). $^{\#}p$ <0.05 and $^{\#\#}p$ <0.01 vs. non-treated control; *p <0.05 and **p <0.01 vs. UVA-irradiated group

Acknowledgment This research was financially supported by the Ministry of Trade, Industry and Energy, Korea, under the "Regional Innovation Cluster Development Program (R&D, P0015361)" supervised by the Korea Institute for Advancement of Technology (KIAT).

References

1. Lee YR, Noh EM, Jeong EY, Yun SK, Jeong YJ, Kim JH, Kwon KB, Kim BS, Lee SH, Park CS, Kim JS (2009) Cordycepin inhibits UVB-induced matrix metalloproteinase expression by suppressing the NF-κB pathway in human dermal fibroblasts. Exp Mol Med 41: 548–554. doi: 10.3858/emm.2009.41.8.060
2. Tomasello B, Malfa GA, Acquaviva R, Mantia AL, Giacomo CD (2022) Phytocomplex of a standardized extract from red orange (*Citrus sinensis* L. Osbeck) against photoaging. Cells 11: 1447. doi: 10.3390/cells 11091447
3. Rittié L, Fisher GJ (2002) UV-light-induced signal cascades and skin aging. Ageing Res Rev 1: 705–720. doi: 10.1016/S1568-1637(02)00024-7
4. Zhang H, Zhang Y, Tong X, Tong X, Gao L, Kang L, Zeng J (2021) The Epigenetic Modification in the Pathogenesis of Skin Photoaging. COJ Nurse Healthcare 7: 760–768. doi: 10.31031/COJNH.2021.07.000659
5. Ansary TM, Hossain MR, Kamiya K, Komine M, Ohtsuki M (2021) Inflammatory molecules associated with ultraviolet radiation-mediated skin aging. Int J Mol Sci 22: 3974–3988. doi: 10.3390/ijms22083974
6. Jin YJ, Ji Y, Jang YP, Choung SY (2021) *Acer tataricum* subsp. *ginnala* inhibits skin photoaging via regulating MAPK/AP-1, NF-κB, and TGFβ/Smad signaling in UVB-irradiated human dermal fibroblasts. Molecules 26: 662. doi: 10.3390/molecules26030662
7. de Jager TL, Cockrell AE, du Plessis SS (2017) Ultraviolet light induced generation of reactive oxygen species. Adv Exp Med Biol 996: 15–23. doi: 10.1007/978-3-319-56017-5_2
8. Choi SJ, Lee SN, Kim K, Joo DH, Shin S, Lee J, Lee HK, Kim J, Kwon SB, Kim MJ, Ahn KJ, An IS, An S, Cha HJ (2016) Biological effects of rutin on skin aging. Int J Mol Med 38: 357–363. doi: 10.3892/ijmm.2016.2604
9. Quan T, He T, Kang S, Voorhees JJ, Fisher GJ (2004) Solar ultraviolet irradiation reduces collagen in photoaged human skin by blocking transforming growth factor-β type II receptor/Smad signaling. Am J Pthol 165: 741–751. doi: 10.1016/S0002-9440(10)63337-8
10. Chandra S, Qureshi S, Chopra D, Shukla S, Patel SK, Singh J, Ray RS (2022) UVR-induced phototoxicity mechanism of methyl N-methylanthranilate in human keratinocyte cell line. Toxicol in Vitro 80: 105322. doi: 10.1016/j.tiv.2022.105322
11. Bae JT, Ko HJ, Kim GB, Pyo HB, Lee GS (2012) Protective effects of fermented citrus unshiu peel extract against ultraviolet-a-induced photoageing in human dermal fibrobolasts. Phytother Res 26: 1851–1856. doi: 10.1002/ptr.4670
12. Mohamed MAA, Jung M, Lee SM, Lee TH, Kim J (2014) Protective effect of *Disporum sessile* D.Don extract against UVB-induced photoaging via suppressing MMP-1 expression and collagen degradation in human skin cells. J Photochem Photobiol B 133: 73–79. doi: 10.1016/j.jphotobiol.2014.03.002
13. Kim H il, Jeong YU, Kim JH, Park YJ (2018) 3,5,6,7,8,3′,4′-heptamethoxyflavone, a citrus flavonoid, inhibits collagenase activity and induces type I procollagen synthesis in HDFn cells. Int J Mol Sci 19: 620. doi: 10.3390/ijms19020620
14. Webb AH, Gao BT, Goldsmith ZK, Irvine AS, Saleh N, Lee RP,

Lendermon JB, Bheemreddy R, Zhang Q, Brennan RC, Johnson D, Steinle JJ, Wilson MW, Morales-Tirado VM (2017) Inhibition of MMP-2 and MMP-9 decreases cellular migration, and angiogenesis in in vitro models of retinoblastoma. BMC Cancer 17: 434. doi: 10.1186/s12885-017-3418-y

15. Quan T, He T, Voorhees JJ, Fisher GJ (2001) Ultraviolet irradiation blocks cellular responses to transforming growth factor-β by down-regulating its type-II receptor and inducing Smad7. J Biol Chem 276: 26349–26356. doi: 10.1074/jbc.M010835200
16. Nam EJ, Yoo G, Lee JY, Kim M, Jhin C, Son YJ, Kim SY, Jung SH, Nho CW (2020) Glycosyl flavones from *Humulus japonicus* suppress MMP-1 production via decreasing oxidative stress in UVB irradiated human dermal fibroblasts. BMB Rep 53: 379–384. doi: 10.5483/BMBRep.2020.53.7.253
17. Hyun HB, Hyeon HJ, Kim SC, Go B, Yoon SA, Jung YH, Ham YM (2021) Anti-melanogenesis effects of *Schizophragma hydrangeoides* leaf ethanol extracts via downregulation of tyrosinase activity. Korean J Plant Res 34: 510–516. doi: 10.7732/KJPR.2021.34.6.510
18. Venditti A, Maggi F, Vittori S, Papa F, Serrilli AM, Cecco MD, Ciaschetti G, Mandrone M, Poli F, Bianco A (2015) Antioxidant and α-glucosidase inhibitory activities of *Achillea tenorii.* Pharm Biol 53: 1505–1510. doi: 10.3109/13880209.2014.991833
19. Hasler A, Gross G-A, Meier B, Sticher O (1992) Complex flavonol glycosides from the leaves of *Ginkgo biloba*. Phytochem 31: 1391–1394. doi: 10.1016/0031-9422(92)80298-S
20. Bilia AR, Ciampi L, Mendez J, Morelli I (1996) Phytochemical investigations of *Licania* genus. flavonoids from *Licania pyrifolia*. Pharm Acta Helv 71: 199–204. doi: 10.1016/0031-6865(96)00009-X
21. Chang SW, Kim KH, Lee IK, Ryu SY (2009) Phytochemical constituents of *Bistorta manshuriensis*. Nat Prod Sci 15: 234–240
22. Oh JH, Kim J, Karadeniz F, Kim HR, Park SY, Seo Y, Kong CS (2021) Santamarine shows anti-photoaging properties via inhibition of MAPK/AP-1 and stimulation of TGF-β/Smad signaling in UVA-irradiated HDFs. Molecules 26. doi:10.3390/molecules26123585
23. Oh JH, Karadeniz F, Kong CS, Seo Y (2020) Antiphotoaging effect of 3,5-dicaffeoyl-epi-quinic acid against UVA-induced skin damage by protecting human dermal fibroblasts in vitro. Int J Mol Sci 21: 1–12. doi:10.3390/ijms21207756
24. Hwang E, Gao W, Xiao YK, Ngo HTT, Yi TH (2019) *Helianthus annuus* L. flower prevents UVB-induced photodamage in human dermal fibroblasts by regulating the MAPK/AP-1, NFAT, and Nrf2 signaling pathways. J Cell Biochem 120: 601–612. doi: 10.1002/jcb.27417
25. Ryu TK, Roh E, Shin HS, Kim JE (2022) Inhibitory effect of lotusine on solar UV-induced matrix metalloproteinase-1 expression. Plants 11: 773. doi:10.3390/plants11060773
26. Lee SH, Yang JH, Park YK, Han JJ, Chung GH, Hahm DH, Choi HD (2013) Protective effect and mechanism of phosphatidylserine in UVB-induced human dermal fibroblasts. Eur J Lipid Sci Technol 115: 783–790. doi: 10.1002/ejlt.201200086
27. Kim YJ, Lee EH, Cho EB, Kim DH, Kim BO, Kang I, Jung HY, Cho YJ (2019) Protective effects of galangin against UVB irradiation-induced photo-aging in CCD-986sk human skin fibroblasts. Appl Biol Chem 40. doi: 10.1186/s13765-019-0443-3
28. Zhao P, Alam MB, An H, Choi HJ, Cha YH, Yoo CY, Kim HH, Lee SH (2018) Antimelanogenic effect of an *Oroxylum indicum* seed extract by suppression of MITF expression through activation of MAPK signaling protein. Int J Mol Sci 19: 760. doi: 10.3390/ijms19030760
29. Kim DE, Chang BY, Ham SO, Kim YC, Kim SY (2020) Neobavaisoflavone inhibits melanogenesis through the regulation of Akt/GSK-3β and MEK/ERK pathways in B16F10 cells and a reconstructed human 3D skin model. Molecules 25. doi: 10.3390/molecules25112683
30. Hong JA, Bae D, Oh KN, Oh DR, Kim Y, Kim Y, Im SJ, Choi E, Lee S, Kim M, Jeong C, Choi CY (2022) Protective effects of *Quercus acuta* Thunb. fruit extract against UVB-induced photoaging through ERK/AP-1 signaling modulation in human keratinocytes. BMC Complement Med Ther 22. doi: 10.1186/s12906-021-03473-1
31. Oh JH, Joo YH, Karadeniz F, Ko J, Kong CS (2020) Syringaresinol inhibits UVA-induced MMP-1 expression by suppression of MAPK/AP-1 signaling in HaCaT keratinocytes and human dermal fibroblasts. Int J Mol Sci 21: 3981. doi:10.3390/ijms21113981
32. Kim M, Park YG, Lee HJ, Lim SJ, Nho CW (2015) Youngiasides A and C isolated from *Youngia Denticulatum* inhibit UVB-induced MMP expression and promote type I procollagen production via repression of MAPK/AP-1/NF-κB and activation of AMPK/Nrf2 in HaCaT cells and human dermal fibroblasts. J Agric Food Chem 63: 5428–5438, doi: 10.1021/acs.jafc.5b00467
33. Darwin JP, Aleksander LS, Shi-Wu Li (1998) Procollagen N-proteinase and procollagen C-proteinase. Two unusual metalloproteinases that are essential for procollagen processing probably have important roles in development and cell signaling. Matrix Biol 16: 399–408. doi: 10.1016/S0945-053X(98)90013-0